Latin American Journal of Solids and Structures
www.lajss.org

A path-following driver/vehicle model with optimized lateral dynamic controller

Abstract
Reduction in traffic congestion and overall number of accidents, especially within the last decade, can be attributed to the enormous progress in active safety. Vehicle path following control with the presence of driver commands can be regarded as one of the important issues in vehicle active safety systems development and more realistic explanation of vehicle path tracking problem. In this paper, an integrated driver/DYC control system is presented that regulates the steering angle and yaw moment, considering driver previewed path. Thus, the driver previewed distance, the heading error and the lateral deviation between the vehicle and desired path are used as inputs. Then, the controller determines and applies a corrective steering angle and a direct yaw moment to make the vehicle follow the desired path. A PID controller with optimized gains is used for the control of integrated driver/DYC system. Genetic Algorithm as an intelligent optimization method is utilized to adapt PID controller gains for various working situations. Proposed integrated driver/DYC controller is examined on lane change manuvers andthe sensitivity of the control system is investigated through the changes in the driver model and vehicle parameters. Simulation results show the pronounced effectiveness of the controller in vehicle path following and stability.

Keywords
driver model, vehicle path following, ADAMS, PID controller and genetic algorithm

Behrooz Mashadi 1[a]
Mehdi Mahmoudi-kaleybar 2[b]
Pouyan Ahmadizadeh 3[a]
Atta Oveisi 4[c]

[a] School of Automotive Engineering, Iran University of Science and Technology, Tehran, Iran
[b] Department of Mechanical Engineering, Parand Branch, Islamic Azad University, Parand, Tehran, Iran
m_mahmoodi_k@iust.ac.ir
[c] School of Mechanical Engineering, Iran University of Science and Technology, Tehran, Iran

1 INTRODUCTION

Remarkable advances achieved in the automotive active safety systems during the recent decades by means of active control and assist drivers to maintain the control of vehicles have resulted in preventing unintended vehicle behavior. In order to improve vehicle stability and steerability, electronic control systems such as direct yaw moment control (DYC), electronic stability program (ESP), active steering including 2 Wheel Steering (2WS) and 4 Wheel Steering (4WS), or active front steering (AFS) have been developed). Nam and Fujimoto (2012) proposed a robust yaw stability control design based on active front steering (AFS) control for in-wheel-motored electric vehicles with a Steer-by-Wire (SbW) system. The proposed control system consisted of an inner-loop controller and an outer-loop tracking controller to achieve control performance and stability. An important issue in chassis control systems is to control the vehicle yaw moment by controlling the lateral vehicle motion variables such as yaw rate and side-slip angle (Tchamna and

Youn, 2013). 4WS and AFS can effectively improve the steerability performance in the linear region of the tire (Hwang et al., 2008). DYC, however, can keep the vehicle stable in critical situations where the tire cornering forces reach saturation (e.g. Yang and Wang, 2009). Vertical dynamic interactions between railway tracks and vehicles has been simulated in (Zakeri and et al (2009)), which calculated deflections, accelerations and forces in various track components, and also an study how parameters such as train speed, axle load, rail corrugations, wheel flats and so on influence the track and vehicle components.

Zhang and Kim (2008) presented an AFS controller that was designed by application of the Quantitative Feedback control Theory (QFT), and was based on the integration of feedback signal from the yaw rate sensor.There are several control methods in the literature for tracking the desired response with a DYC system (e.g. Ghoneim et al., 2000, Mirzae et al., 2008, Li et al., 2011, Bang et al., 2001). Esmailzadeh et al. (2003) designed optimal and semi-optimal controllers to improve vehicle handling and stability capabilities. It was shown that the performance of the optimal control law was improved in various aspects; however, those obtained with the semi-optimal control law, which is based on the yaw rate feedback and the steer angle feed-forward is also acceptable for this specific issue. The optimal controller law requires an additional feedback control loop (lateral velocity) that makes the control system even more complex and expensive.
Mashadi and Majidi (2009) designed a yaw moment control system based on the optimal control method which was developed to improve vehicle response in critical situations using a four degrees-of-freedom (4-DOF) linear vehicle model instead of a basic bicycle model. The external yaw moment was achieved by implementation of two electric motors integrated into each of the drive wheels and were controlled independently to control the yaw rate and lateral speed of the vehicle. Mokhiamar and Abe (2002) considered cooperation of 4WS and DYC to maximize stability as well as vehicle responsiveness during severe maneuvers for active vehicle handling safety. They used a linear 4WS controller which was designed independent of the DYC controller. In the work of Wei and Zhuoping (2009) an integrated AFS and DYC chassis control system was presented using fuzzy logic controller to properly distribute the required yaw moment between the AFS and DYC control systems.

An optimal control law was proposed by Goodarzi et al. (2006) to control the vehicle path by regulating variables such as the yaw rate, lateral velocity, lateral offset, and the heading error. Start and aim point of the desired track was specified for the integrated control system to provide both the front steering angle and the external yaw-moment signals as the control efforts. An Active vibration control using PID controller has been proposed by Rahman et al. (2012), the experimental results obtained by using the active vibration control system have demonstrated the validity and efficiency of PID controller.
It is a common practice in the early stages of the development to evaluate a control system on a theoretical vehicle model before evaluating it on an actual vehicle. A more realistic model uses a driver model as well as the vehicle model (Raksincharoensaka et al., 2010). McRuer and Krendel (2007) proposed a quasi-linear model describing the human by means of a linear second-order differential equation with dead time. Then McRuer et al. (2010) modified this feedback driver model, which includes transfer function with lead-lag time constants and time delay to characterize a driver's behavior. These constants can be regulated by crossover frequency assumption and fitting test data. A more complex transfer function model was presented by Hess and Modjtahedzadeh (1990), which described the driver's behavior at low and high frequencies. Several driver models for vehicle lateral control, which are based on optimal control methods, can be found in the literature, e.g. driver models based on the preview-follower theory (Gazis et al., 1961), pure closed-loop predictive control models (Cole et al., 2006) and two- or three-layer preview models (Oscarsson, 2003). An optimal preview control method is applied to the automobile path planning problem by Li and Song (2012) which uses a comprehensive driver model. The well-known MacAdam's driver model was first presented in MacAdam (1981). Starting with the

preview control concept, the MacAdam's model provides an optimal solution for selecting state feedback gains. This model performs very well for normal lateral driving behaviors. R.S. Sharp et al. (2005) proposed a mathematical nonlinear model for the steering control of an automobile. Hermannstädter and Yang (2012), Moon and Choi (2011) intend to introduce a real-world driving experiment model with focus on controlling the variation of steering and lane keeping behavior The steering angle is deduced by utilizing lateral offset and heading angle. Chatzikomis and Spentzas (2009) without modeling of driver behavior assumed that the driver performs a PID control in order to follow the path. Therefore, a combined longitudinal-lateral controller that was regulating the steering angle and throttle/brake levels by previewing the path ahead of the vehicle according to PID controller was presented.

In the current research, a driver model is integrated with a vehicle model aiming at a more realistic representation of the vehicle system. In this way, to improve vehicle path following and stability condition the integration of the AFS/DYC controller, with the consideration of driver inputs is proposed. The main contribution is an intelligent controller based on the driver path preview model. Furthermore, a yaw moment control system based on the optimal PID control method which is optimized by genetic algorithm (GA) is integrated with the driver/vehicle system. The aim is to develop a path-following driver model, which minimizes lateral deviation and heading error according to previewed path (driver intended path) and improves stability conditions by regulating yaw and lateral velocities during various maneuvers. For this purpose, stability analyses are presented, then the controller performance is illustrated in lane change maneuvers.

2 Vehicle Mathematical Model

In this study, two types of vehicle dynamics models have been developed for vehicle path following analysis and improvement of vehicle handling properties. The first model is a simple linear vehicle model that incorporates a driver model which is used for controller design. The second vehicle model is an 8 DOF nonlinear model for control system evaluation through computer simulations. The degrees of freedom associated with this model are the longitudinal velocity U, the lateral velocity V_y, the yaw rate r, the roll rate $\dot{\phi}$, and the wheels rotational speeds, ω_{fl}, ω_{fr}, ω_{rl}, and ω_{rr}. In this paper, to simulate the control of a vehicle during path fallowing in various maneuvers, a typical FWD, front wheel steering passenger car that includes both lateral and longitudinal dynamics is being used.

2.1 Steering System Model

The flexibility of the steering column and steering linkages together with the mass and inertia available in the system makes it prone to vibration. This can affect the driver's commands for path following. So, as shown in Fig. 1, the steering system model can mathematically be expressed by the following equation first introduced by Segel (1982):

$$(I_{sw} + I_s)(\ddot{\delta}_f + \dot{\theta}) = -K_{ss}(\delta - \theta / N) + \frac{\partial \delta_f}{\partial \Phi} K_{ss} \Phi + C_{sw} \dot{\delta}_f + M_z - X_r F_{yf} \tag{1}$$

where, I_{sw} and I_s are equivalent moment of inertia of the handwheel and the steerable wheels respectively, M_z and F_{yf} are the lateral force and self-aligning torque of front axle, X_r is the mechanical trail, N is the steering gear ratio from the handwheel to the road wheels, Φ is the vehicle roll angle, ϑ and δ_f are the input steering wheel angle and the front wheel steering angle respectively.

K_{ss} and C_{ss} are the equivallent stiffness and damping between the road wheels and the steering mechanism.

2.2 Tire Model

Due to the interaction between the longitudinal and lateral tire forces during high lateral acceleration situations, Pacejka's combined slip Magic Formula tire model in Pacejka (2002) is considered here. The tire forces and moments can be expressed as:

$$[F_{wxi}, F_{wyi}, M_{zi}] = f(\lambda_i, \alpha_i, \gamma_i, F_{zi}) \tag{2}$$

where, F_{wxi} and F_{wyi} are the longitudinal and lateral tire forces, M_{zi} is the tire self-aligning moment and f is a non-linear function of the tire's longitudinal slip λ_i, the slip angle α_i, the camber angle γ_i, and the vertical load F_{zi}.

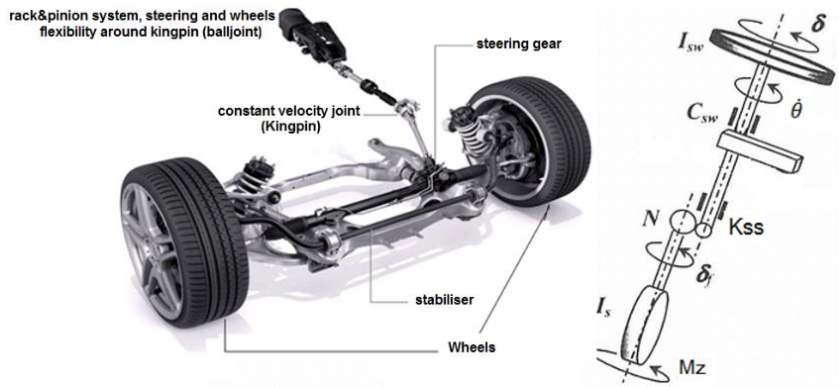

Fig.1 Steering system mechanism (Rosettes 2003)

3. Controller Design

The purpose of control system is to ensure that the vehicle follows a desired path with yaw rate and side-slip angle close to their desired values and with the application of a minimum external yaw moment. Also, the controller is expected to perform at the presence of driver commands. The schematic diagram of the proposed controller in Fig. 2 is representative of a typical driving situation where a vehicle should track a desired path.

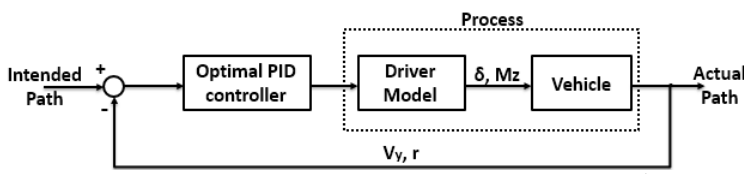

Fig.2 Path following controller structure for closed loop driver/vehicle system

In order to control a vehicle to follow a desired path, one should develop a mathematical model for the vehicle lateral dynamics and express the relationship between the vehicle and the desired path. The dynamics of the vehicle in the controller system is modeled by a 2-DOF linear bicycle

model as shown in Figure 3, which represents the lateral vehicle dynamics in the linear handling region. The standard form of this model is available in the literature, for instance Mirzae et al. (2008), Li et al. (2011). The equations of vehicle dynamics can be described as follows:

$$M(\dot{V}_y + Ur) = F_{yr}\cos\delta_r + F_{xr}\sin\delta_r + F_{yf}\cos\delta_f + F_{xf}\sin\delta_f \tag{3}$$

$$I_z\dot{r} = aF_{yf}\cos\delta_f + aF_{xf}\sin\delta_f - bF_{yr}\sin\delta_r - bF_{yr}\cos\delta_r \tag{4}$$

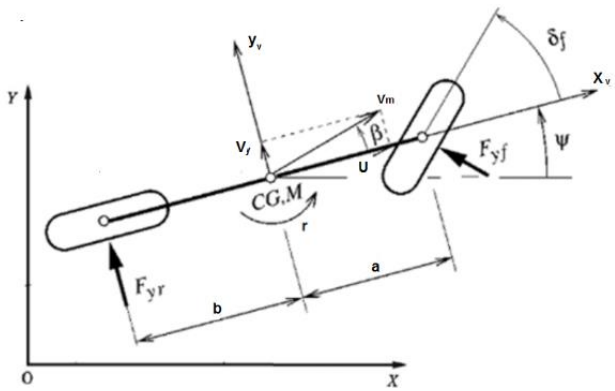

Fig. 3 Vehicle 2-DOF bicycle model

where, M is the vehicle mass, I_z is the moment of inertia of the vehicle, a and b are the distances from the center of gravity to the front and rear axles, respectively, F_{yf} is the lateral tire force of the front wheels, F_{yr} is the lateral tire force of the rear wheels, U and V_y are longitudinal and lateral velocities of CG, r is yaw rate of the vehicle, δ_f and δ_r are the front and rear steering angles, respectively.

According to Fig.4 the heading error (ψ) and the lateral deviation (y_e) of the vehicle are related to the desired path and are combined with the 2-DOF vehicle model as follows:

$$\dot{y}_e = U\sin(\psi) + V_y\cos(\psi) \tag{5}$$

$$\dot{\psi} = \dot{\psi}_\upsilon - \dot{\psi}_r \tag{6}$$

where indices V_y and r are the representative of vehicle and road, respectively and $\dot{\psi}_r$ is defined as the road curvature rate which equals to the longitudinal velocity divided by the radius of the road curvature, (U/R).

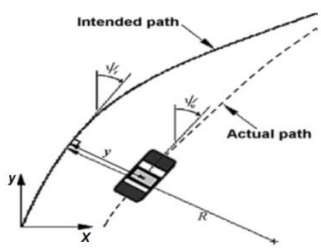

Fig.4 Vehicle parameters in relation to path position of vehicle in (Micheau and Bourassa 2009)

The system equations can be described by the following state space representation based on assumptions of small heading angle error and a constant longitudinal vehicle speed U:

$$\dot{X}_1 = A_1 X_1 + E_1 \delta + B_1 M_z + K(1/R(t)) \tag{7}$$

$$X_1 = \begin{bmatrix} y_e \\ V_y \\ \psi \\ r \end{bmatrix} \quad A_1 = \begin{bmatrix} 0 & 1 & U & 0 \\ 0 & a_{11} & 0 & a_{12} \\ 0 & 0 & 0 & 1 \\ 0 & a_{21} & 0 & a_{22} \end{bmatrix} \quad E_1 = \begin{bmatrix} 0 \\ e_1 \\ 0 \\ e_2 \end{bmatrix} \quad B_1 = \begin{bmatrix} 0 \\ 0 \\ 0 \\ b \end{bmatrix} \quad K = \begin{bmatrix} 0 \\ 0 \\ -U \\ 0 \end{bmatrix} \tag{8}$$

where,

$$\begin{cases} a_{11} = -2\dfrac{C_{\alpha f} + C_{\alpha r}}{MU} \quad a_{12} = -2\dfrac{bC_{\alpha r} + C_{\alpha f}}{MU} - U \quad a_{21} = 2\dfrac{bC_{\alpha r} - \alpha C_{\alpha f}}{I_z U} \\ a_{22} = -2\dfrac{a^2 C_{\alpha f} + b^2 C_{\alpha r}}{I_z U} \quad e_1 = 2\dfrac{C_{\alpha f}}{M} \quad e_2 = -2\dfrac{aC_{\alpha f}}{I_z} \end{cases} \tag{9}$$

In equation 9, $C_{\alpha f}$ and $C_{\alpha r}$ are the cornering stiffness of the front and rear tires respectively which are the slopes of tire forces with respect to variation of slip angles.
For the vehicle model, the lateral velocity v and the yaw rate r are considered as the two state variables while the yaw moment M_z is the control input, which must be calculated through the control law. Furthermore, the vehicle steering angle δ is considered as the external disturbance which is controlled by the driver model.

3.1 Driver Model

The driver model proposed here is a modified version of the mathematical models of an ideal driver presented by Rosettes (2003) and Li et al. (2012). This driver model is based on a the path-following concept which invloves several terms including proportional coefficient (h), preview of the road path (lead constant, τ_1), reaction and delay times (τ_r and τ_d) and vehicle relocating during deviation (lag constant, τ_2). The human driver transfer function is given by:

$$H(s) = \frac{\Delta(s)}{E_d(s)} = \frac{h}{N}\left[\frac{\tau_1 s + 1}{\tau_2 s + 1}\right]\left[\frac{1}{\tau_r s + 1}\right] e^{-\tau_d s} \tag{10}$$

where, $\Delta(s)$ and $E_d(s)$ are the Laplace transforms of δ and the preview tracking error (y_{ep}), respectively. The lateral deviation, which is used by the driver, can be expressed as:

$$y_{ep} = y_e + L\psi \tag{11}$$

In the above equation, y_e is the lateral offset and ψ is the heading angle, and L is a preview distance. In other words, vehicle previews the lateral deviation which must be compensated by the

driver and controller cooperation. In the equation (10), the transportation lag term $e^{-\tau_d}$ is approximated by the first-order Pade polynomial:

$$e^{-\tau_d s} = \left[\frac{1-\frac{\tau_d}{2}s}{1+\frac{\tau_d}{2}s}\right] \tag{12}$$

Therefore, the human driver equation can be obtained using equations (10) and (12) in the time variant space in the form bellow:

$$\ddot{\delta}=w\left[-(\ddot{y}_e+L\ddot{\psi})+2\frac{\tau_1}{\tau_2}(\dot{y}_e+L\dot{\psi})\right]+(y_e+L\psi)]+\frac{1}{\tau_n.\tau_2}[-(\tau_n+\tau_2)\dot{\delta}-\delta] \tag{13}$$

where, W is the constant coefficient of defined as:

$$W = \frac{h}{N}.\frac{1}{\tau_n.\tau_2} \tag{14}$$

3.2. Close

d Loop Driver/Vehicle Model

The integrated closed loop zdriver/vehicle model in a state-space form is given by:

$$\dot{X} = AX + BM_z + K[1/R] \tag{15}$$

where,

$$X=\begin{bmatrix} ye \\ v \\ \psi \\ r \\ \delta \\ \dot{\delta} \end{bmatrix} \quad A=\begin{bmatrix} 0 & 1 & 0 & 0 & 0 & 0 \\ 0 & a_{11} & 0 & a_{21} & e_1 & 0 \\ 0 & 0 & 0 & 1 & 0 & 0 \\ 0 & a_{21} & 0 & a_{22} & e_2 & 0 \\ 0 & 0 & 0 & 0 & 0 & 1 \\ a_{16} & a_{62} & a_{63} & a_{64} & a_{65} & a_{66} \end{bmatrix} \quad B=\begin{bmatrix} 0 \\ 0 \\ 0 \\ b \\ 0 \\ Wb \end{bmatrix} \quad K=\begin{bmatrix} 0 \\ 0 \\ -U \\ 0 \\ 0 \\ -WU^2-\frac{2W\tau_1}{\tau_d}LU \end{bmatrix} \tag{16}$$

$$\begin{cases} a_{61} = W \quad a_{62} = W(a_{11} + La_{21}) + \dfrac{2W\tau_1}{\tau_d}, \quad a_{63} = -\dfrac{2W\tau_1}{\tau_d}U + WL \\ a_{64} = W(a_{21} + La_{22} + U) + \dfrac{2W\tau_1}{\tau_d}L, \quad a_{65} = \dfrac{-1}{\tau_n.\tau_1} + e_1 + Le_2, \quad a_{66} = \dfrac{(\tau_n + \tau_2)}{\tau_n.\tau_2} \end{cases} \tag{17}$$

3.3 Development of Control Law

Owing to its simple practical nature, PID type controllers shown in Fig.5 are developed for the lateral and longitudinal directions of the vehicle path following problem. The yaw moment control law for the desired state space vector $X_d = [y_d \; v_d \; \psi_d \; r_d \delta\dot{\delta}_d]^{\mathrm{T}}$ is achieved by this control system.The transfer function of a PID controller is described as follows:

$$G_c(s) = k_p + \frac{k_i}{s} + k_d s \tag{18}$$

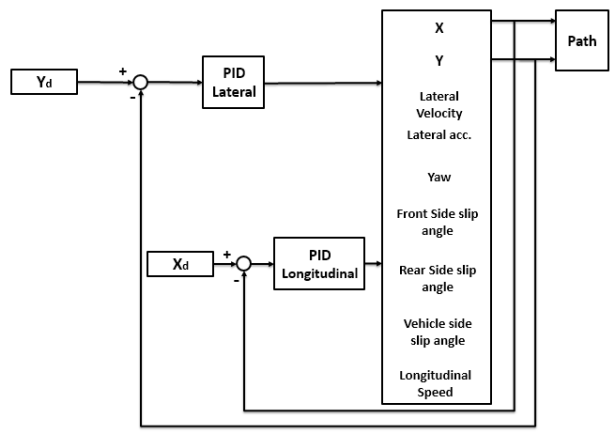

Fig.5 Lateral and longitudinal PID controller

where, k_p, k_i and k_d are proportional, integral and derivative gains, respectively. A set of optimized control parameters can make an appropriate step change responses of driver/vehicle state variables, which will result in performance criteria minimization. Performance criterion in the time domain includes parameters such as overshoot M_p, steady state error E_{ss}, rise time t_r, and settling time t_s. Moreover, to enhance optimal controller gains, which can make the controller more robust and efficient, an intelligent optimization is utilized by the application of Genetic Algorithm method to adapt controller parameters for any driving style and road condition.

3.4. Implementing GA for Design of PID Gains

In PID controller design, the main issue is to find the best values for k_p, k_i and k_d which in classic methods, needs considerable computer simulation efforts in a time-consuming trial and error process. Thus, using intelligent optimization methods for finding them is more attractive. Fig. 6

illustrates a process by which the genetic algorithm (GA), as a powerful and broadly applicable stochastic search and optimization technique, is used to optimize the PID controller to obtain the most appropriate gains. This process will be called PID-GA. It can be considered as a family of computational models inspired on the principals of evolution. Castro and Partridge (2006) proposed the proceure of using GA operatores, by considering dynamic analysis.

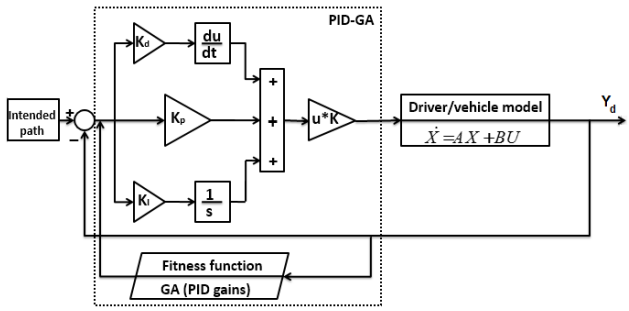

Fig.6 Block diagram of GA optimization process for the PID controller

The application of GA to the PID controller must make the closed-loop system (i) as fast as possible and (ii) as stable as possible, using (iii) as lowest control effort as possible and as minimum overshoot as posible (Ghoreishi, 2011).

Stability Index. This index is related to real parts of closed-loop poles ($\varkappa$) and is defined as follows:

$$SI = -\frac{1}{\max \mathrm{Re}\{\kappa_i\}} \tag{19}$$

Obviously, the improved PID gains give smaller stability index.

Settling-time Index. For a time response of a system, this index is the minimum time during which, the response reaches the absolute error of 0.05. In the mathematical form:

$$ST = \min\left\{t \left| \frac{y(t) - y_d(t)}{y_d(t)} \le 0.05 \right.\right\} \tag{20}$$

where, $y\ (t)$ is the time response and $y_d\ (t)$ is the desired output trajectory.

Maximum Control Effort Index. Due to the limitations of actuators, the objectives should be usually satisfied with minimum control efforts. Maximum control effort of the system can be de

fined a

s:

$$u_{\max} = \max|u(t)| \tag{21}$$

where, $u(t)$ is the controller input that includes external moment in this paper. Finding the best values for k_p, k_i and k_d by using the above indices is a multi-objective optimization problem. Therefore, fitness function, which should be minimized by GA, can be written with regard to the closed-loop response (Oliveira, 2010, Schoen, 2009):

$$I = {t_r}^{0.2} + {t_s}^{0.5} + {E_{ss}}^{5} + {M_p}^{2} \tag{22}$$

The exponents of Equation 22 are adjusted in such a way that the transient response properties namely rise time (t_r), settling time (t_s), steady-state error (E_{ss}) and overshoot all attain lower values.

4. Results

In order to analyze the performance of the combined control system, computer simulation is performed utilizing the nonlinear driver-vehicle model.

In the first step, nonlinear vehicle model verification is carried out. Then, stability analysis for the open loop and closed loop systems were proposed with and without the controller. Finally, computer simulations are carried out in a double lane change maneuver. Moreover, sensitivity analysis of vehicle parameters and look ahead distance on vehicle path following are presented.

4.1 Vehicle Model Verification

The closed loop vehicle model developed in Matlab/Simulink environment is verified by using ADAMS software results. Fig. 7 shows the comparison results of a lane change maneuver simulation of the proposed model with those of the ADAMS software in the same conditions, showing side slip angle and lateral acceleration, respectively.

The proposed model results in good accuracies for lateral acceleration and side slip angle in a lane change maneuver. But, a small error is observed due to ignoring the suspension kinematics and compliance effects.

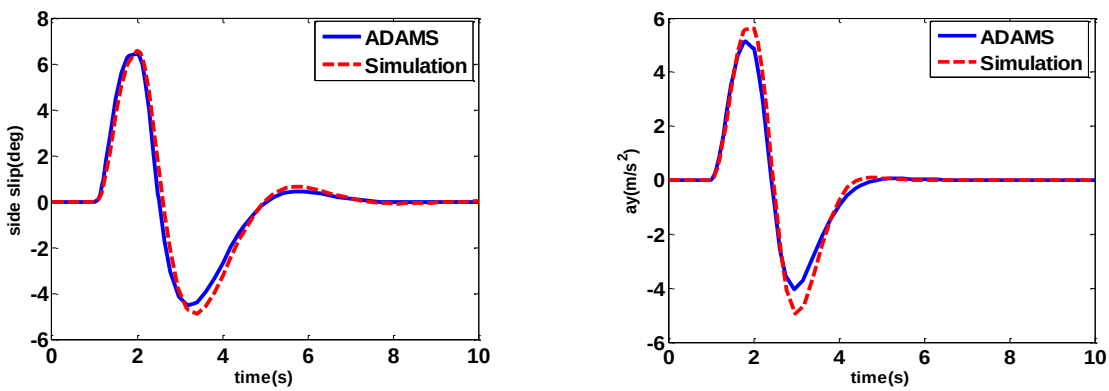

a) Side slip angle b) Lateral acceleration

Fig.7 Vehicle model verification via ADAMS software during a lane change maneuver

4.2 Stability Analysis

It is evident that stability of the closed-loop driver/vehicle system in the state-space form can be judged by pole placement and response of the open and closed loop systems. Therefore, step responses of the open and closed loop systems are used as the evaluation criteria of the control efficiency. Step responses of the open and closed loop systems with PID and PID-GA controllers are illustrated in Figs. 8 and 9, respectively.

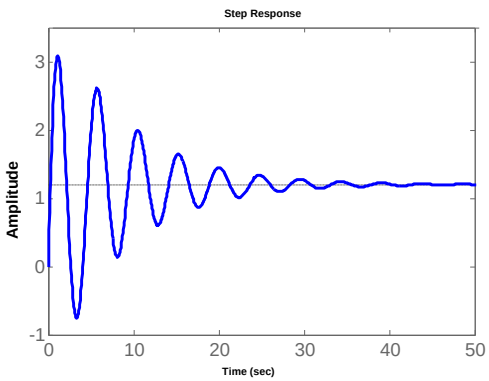

Fig.8 Open-loop step response without controller

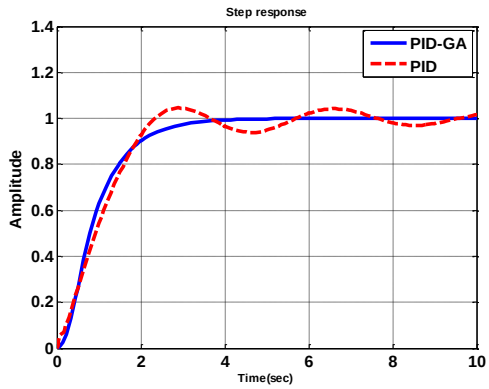

Fig.9 Closed-loop step response with controller

Based on the step responses presented in Figs. 8 and 9, it is seen that the open loop system without driver/controller cannot be considered as an acceptable system. Application of the integrated driver/DYC controller improves the response of the system. The system response is further improved by applying the genetic algorithm which optimizes PID gains and shows that the optimization indices which include rise time and overshoot, are minimized.

Open loop system without driver includes four poles such as lateral deviation, heading error and their rate, which two of them are positive that make the system unstable. Closed loop system with driver model has two more poles which are steering angle and its rate. Additional poles make the system stable. Figs. 10 and 11 illustrate the comparison between PID-GA and PID for stability index through Root locus plots. It is observed that the genetic algorithm in PID method modifies the stability index.

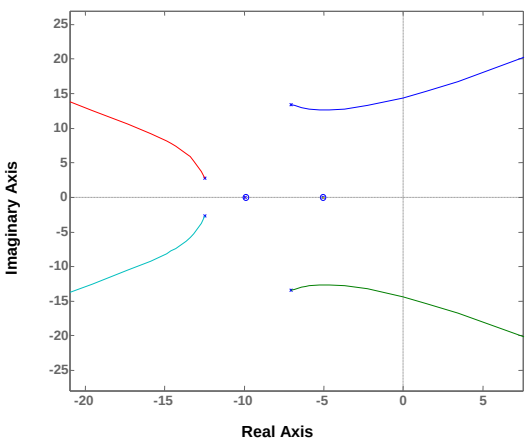

Fig.10 Root locus with PID-GA

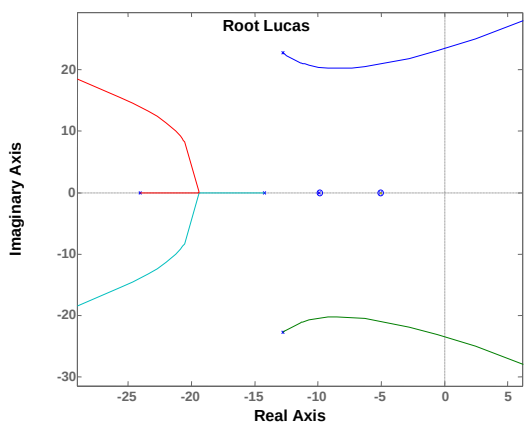

Fig.11 Root locus with PID

Furthermore, to analyze the stability of the PID and PID-GA, the real part of the unstable pole in the open loop system has been plotted as a function of velocity for both cases in Fig.12.

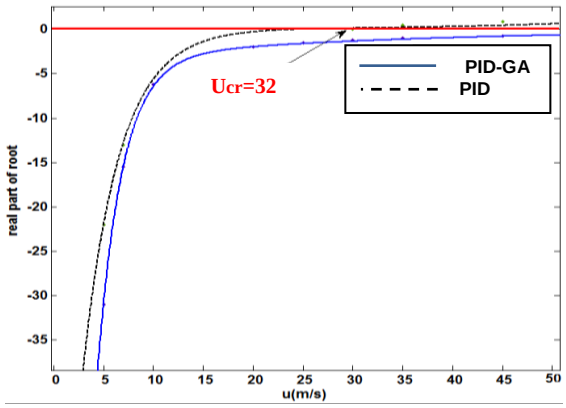

Fig.12 Real parts of the PID and PID-GA critical pole versus velocity

The original uncontrolled vehicle is an oversteer case in Figure 12. This figure indicates that the PID controller is unable to restore stability at vehicle speeds higher than the critical speed of 32 m/s. Whereas, the optimized PID-GA controller shows stability at all practical vehicle speeds.

4.3 Simulation Results

Digital simulations were carried out using double lane-change maneuver at a constant speed of 80 km/h to analyze the performance of the combined control system of the Driver/DYC as an intelligent control system and to compare the performance improvements produced by the proposed PID-GA and the PID methods.

Fig. 13 shows the simulation results for the vehicle dynamics behavior during path following on a double lane-change maneuver. Desired path and state space variables are shown in Figs. 13 a, b, c, d and e, respectively. Also, the applied external yaw moment and the front steering angle, as the control efforts, are shown in Figs.12 f and g, respectively. The results indicate that both controllers have improved the path following performance of the vehicle in comparison to the uncontrolled one. Moreover, the results of the PID-GA controller showed better responses than those of the classic controller.

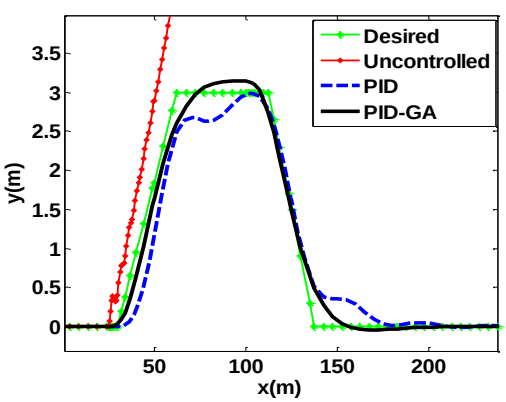

a)Double lane change maneuver path

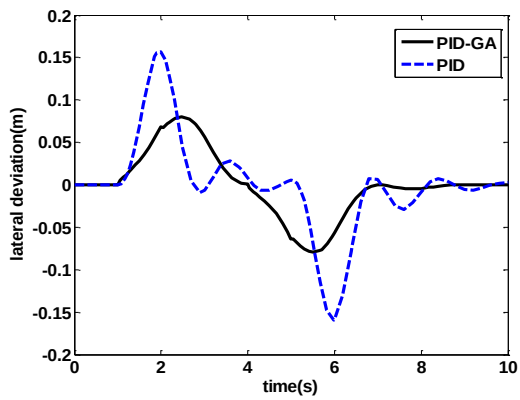

b) Lateral deviation

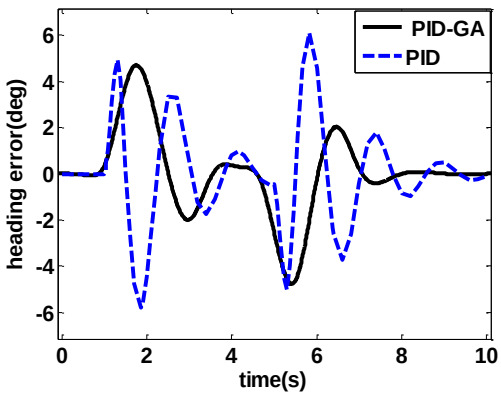

c) Heading error angle

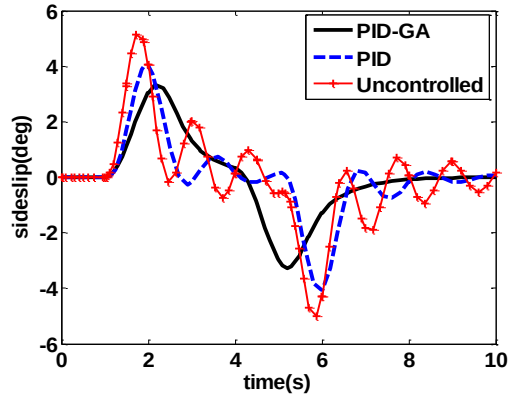

d) Side slip angle

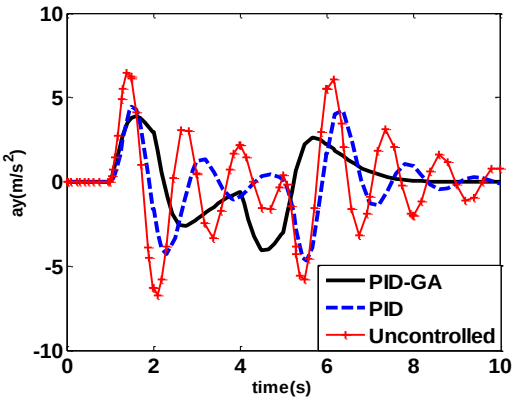

e) Lateral acceleration

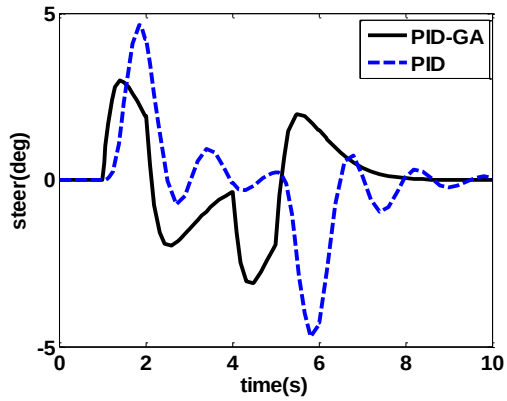

f) Driver steering angle (control effort)

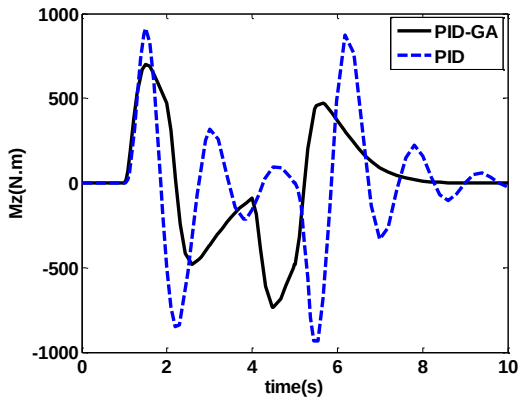

g) Direct yaw moment (control effort)

Fig.13 Simulation results during the double lane change maneuver

The vehicle double lane change in Fig. 13a shows that the uncontrolled vehicle cannot follow the desired path, whereas the PID-GA controller was capable to change the lane smoother than the PID one, and follows driver intended path with less lateral deviation and heading errors. Furthermore, side slip angle and lateral acceleration responses indicate that the control system has quicker responses with lower errors, while, the uncontrolled system becomes unstable in critical conditions.

4.4 Sensitivity Analysis

The vehicle motion is affected by the vehicle's inherent dynamics and the human driver's control characteristics expressed by the driver model transfer function *H(s)*. In order to study the sensitivity of vehicle motion, a target lane-change maneuver is defined. In this section, the robustness and sensitivity of the control system has been investigated through the changes in the driver previewed path and vehicle parameters.

4.4.1 Driver Model Properties and Previewed Path

It is clear that for a closed-loop driver/vehicle system, there is a lower limit of the driver's preview distance. This limit is due to the response delay of the driver and the critical preview distance, which is equal to the distance the vehicle moves with speed u, during the driver delay and reaction time (τ_d and τ_r). Also, the driver must focus on the target path which results in an upper limit of look-ahead distance that can make the system oscillatory. To evaluate the previewed path effect on path tracking, as shown in Fig.14, changes in the look-ahead distance L, during the lane change maneuver has been considered.

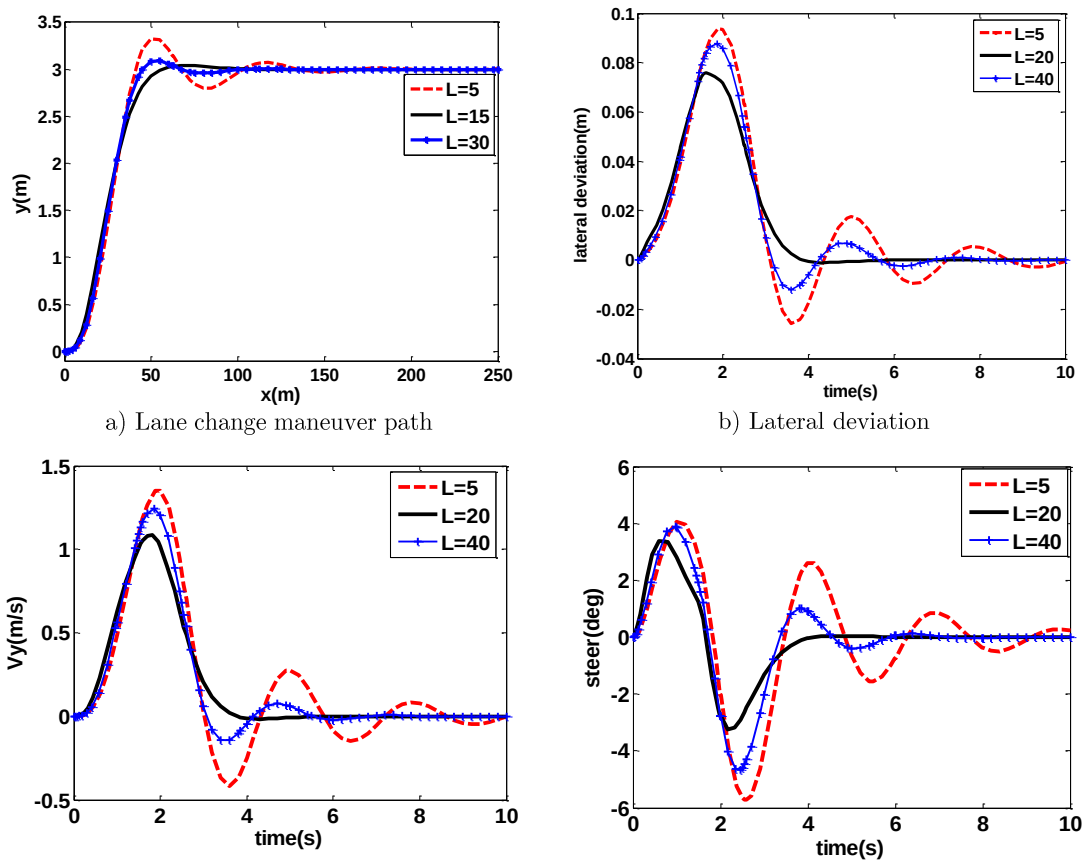

a) Lane change maneuver path

b) Lateral deviation

c) Lateral velocity

d) Driver steering angle

Fig. 14 The effect of driver's look-ahead distance on path following during the lane change maneuver

There is an optimized range for look-ahead distance according to the driver/vehicle properties which can affect path following and stability. Nonetheless, it is obvious that the utilized DYC controller reduced driver workload and path deviation.

4.4.2 Vehicle Parameters

The robustness of the control system has been investigated through the changes in the vehicle parameters. The results indicate that the cornering stiffness of the tires and center of gravity are the most important parameters that affect the performance of the control system. Path following and state space variables are illustrated in Fig.15 for four cases: understeer, neutral steer, oversteer and sever oversteer vehicles.

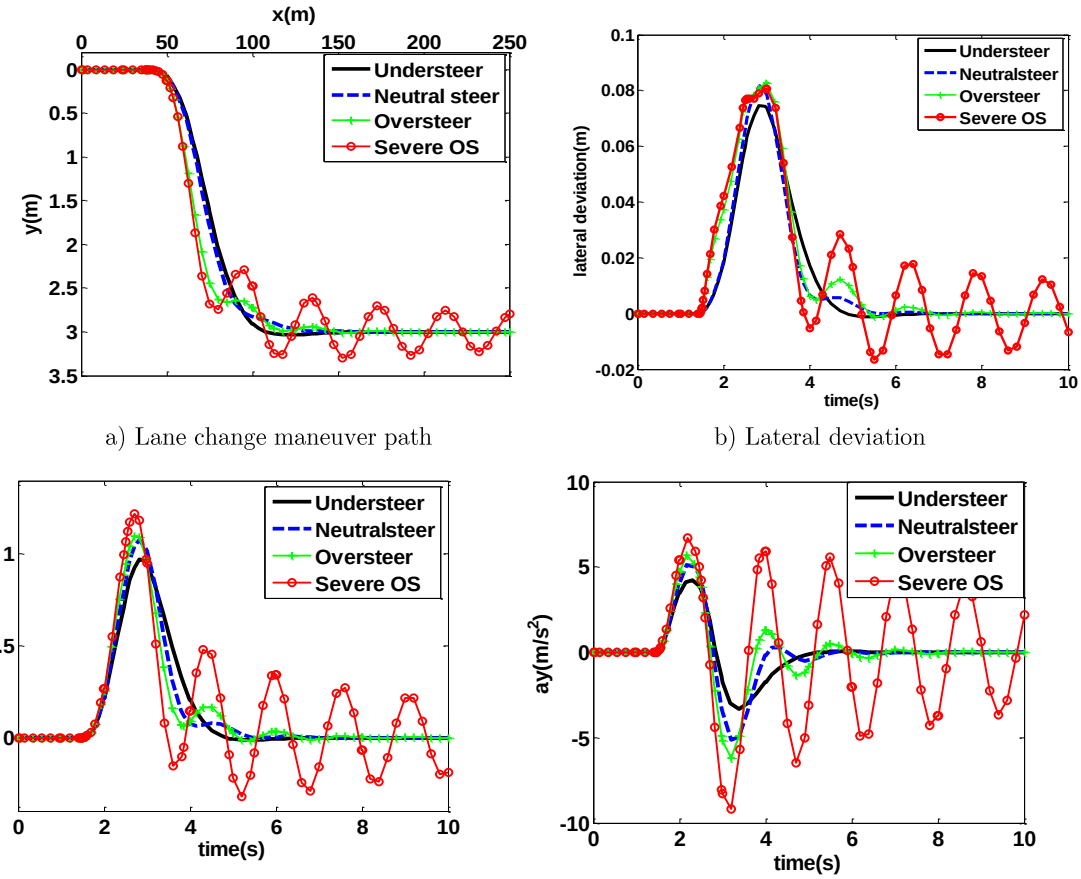

a) Lane change maneuver path

b) Lateral deviation

c) Heading error

d) Driver steering angle

Fig.15 Effect of vehicle understeer/oversteer properties on the lane change path following

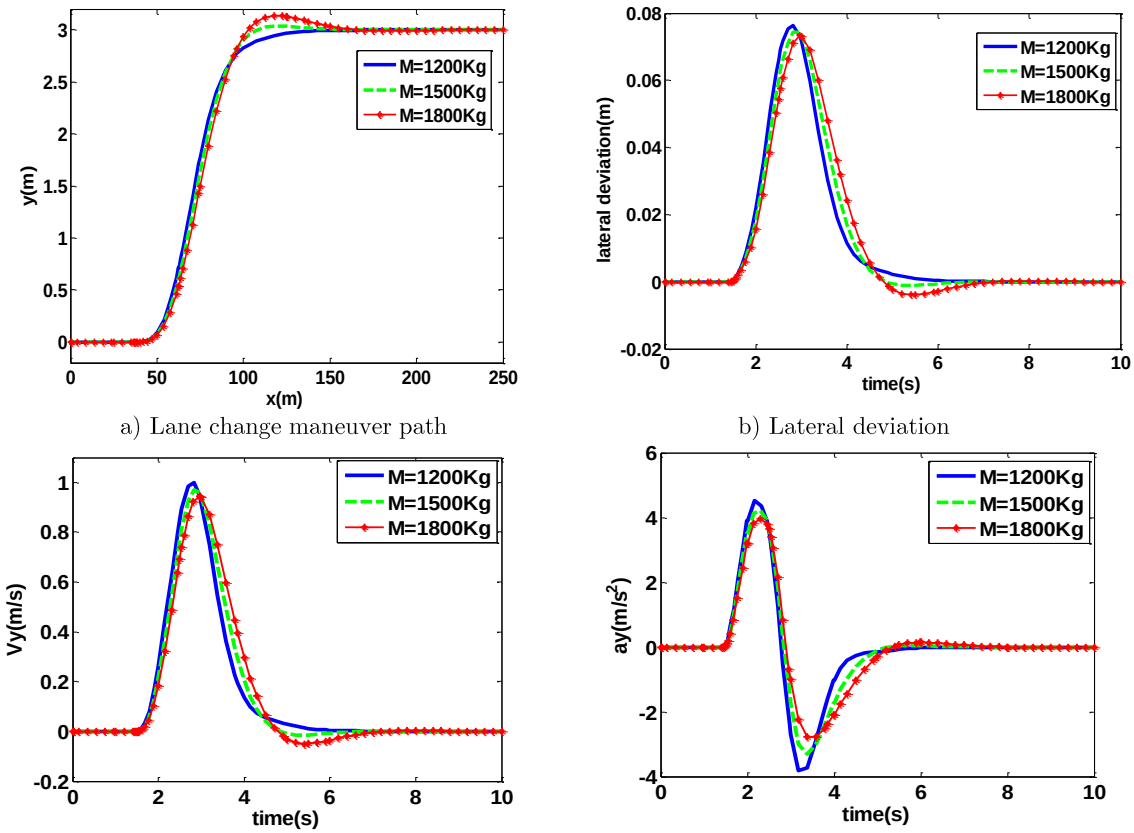

a) Lane change maneuver path

b) Lateral deviation

c) Heading error

d) Driver steering angle

Fig.16 Various vehicle's mass effect on vehicle path following

5. Conclusion

In this study, in order to make the vehicle to follow the desired path, the effectiveness of the direct yaw moment control with PID and PID-GA theories were evaluated in the driver/vehicle closed-loop system. The proposed control law is developed based on tracking the previewed path, vehicle yaw rate and lateral velocity. For this purpose, a number of simulations were conducted with a nonlinear driver/vehicle closed-loop model for single and double lane change maneuvers. Vehicle stability, handling and path tracking performances were compared in three uncontrolled, PID and PID-GA controlled cases. Simulation results clarified that the closed-loop driver vehicle response was stable even under severe maneuvers in which an open-loop vehicle is unstable. Moreover, PID-GA path following controller showed a clear improvement in the vehicle stability compared to the cases of PID and without DYC, and had minimum lateral deviation and heading errors along driver's intended path.

In order to analyze the robustness of the path-following controller in regard to the changes in driver properties and vehicle parameters, genetic algorithm was applied. Results indicated that the designed controller is still stable and presents good tracking performance to the driver's intent for different running conditions. In other words, integrated driver/DYC control is adaptive to different driving conditions.

References

Bang, M.S., Lee, S.H., Han, C.S., and et al., (2001), "Performance Enhancement of a Sliding Mode Wheel Slip Controller by the Yaw Moment Control", Proc. IMechE Part D: J. Automob. Eng. 215 (4), 455–468.

Castro, L.C.L.B., Partridge, P.W., (2006), "Minimum weight design of framed structures using a genetic algorithm considering dynamic analysis", Latin American Journal of Solids and Structures, Volume 3, 107-123

Chatzikomis, C.I., Spentzas, K.N., (2009), "A Path-Following Driver Model With Longitudinal and Lateral Control of Vehicle's Motion", Forschung im Ingenieurwesen, Vol. 73, No. 4., pp. 257-266.

Cole, D. J., Pick, A. J., Odhams, A.M.C., (2006), "Predictive and Linear Quadratic Methods for Potential Application to Modeling Driver Steering Control", Vehicle system Dynamic, 44_3_, pp. 259–284.

Esmailzadeh, E., Goodarzi, A., Vossoughi, G.R., (2003), "Optimal Yaw Moment Control Law For Improved Vehicle Handling", Elsevier Science Ltd, Mechatronics 13, 659–675.

Gazis, D. C., Herman, R., Rothery, R.W., (1961), "Nonlinear follow-the-leader models of traffic flow", Operations Research, Vol. 9, no. 4, pp. 545-567.

Ghoneim, Y.A., Lin, W.C., Sidlosky, D.M., and et al., (2000), "Integrated Chassis Control System to Enhance Vehicle Stability", Vehicle system Dynamic. 23 (1/2), 124–144.

Ghoreishi, S.A., Nekoui, M.A., Basiri, S.O., (2011), "Optimal Design of LQR Weighting Matrices based on Intelligent Optimization Methods", Int. J. of Intelligent Information Processing, Vol. 2, Num.1.

Goodarzi, A., Sabooteh, A., Esmailzadeh, E., (2006), "Automatic Path Control Based on Integrated Steering and External Yaw-Moment Control", Proc. IMechE Part K: J. Multi-body Dynamics, Vol. 222.

Hess, R.A., Modjtahedzadeh, A., (1990), "A Control Theoretic Model of Driver Steering Behavior", Control System Magazine, IEEE, Vol. 10, Iss: 5, pp. 3-8.

Hermannstadter, P., Yang, B., (2012), "Identification and Validation of Lateral Driver Models on Experimentally Induced Driving Behavior", Systems, Man, and Cybernetics (SMC), IEEE International Conference on, vol., no., pp.1165-1170, 14-17 Oct.

Hwang, T. H., Park, K., Heo, S. J., Lee, S. H. and Lee, J. C., (2008), "Design of integrated chassis control logics for AFS and ESP", International Journal of Automotive Technology, Vol. 9, No. 1, pp. 17-27.

Jorgensen, T., (2007), "Modeling Driver Behavior in Automotive Environments", Critical Issues in Driver Interactions with Intelligent Transport Systems. London: Springer.

Jazar R., (2008), "Vehicle Dynamics Theory and Application", Springer Science+Business Media, LLC, 2nd Edition.

Leelavansuk, P., Yoshida, H., Nagai, M., (2003), "Cooperative Steering Characteristic of Driver and Lane-Keeping Assistance System", International J. of ITS Research, Vol.1, No.1.

Li, H. Z., Li, L., Song, J. and Yu, L. Y., (2011), "Comprehensive lateral driver model for critical maneuvering conditions" International Journal of Automotive Technology, Vol. 12, No. 5, pp. 679−686.

MacAdam, C.C., (1981), "Application of an Optimal Preview Control for Simulation of Closed-loop Automobile Driving", IEEE Transactions on systems, man, and cybernetics, Vol. SMC- II, No. 6, pp. 393-399.

Mashadi, B., Majidi, M., Pourabdollahdizaji, H., (2009), "Optimal Vehicle Dynamics Controller Design Using a Four-Degrees-of-Freedom Model", Proc. IMechE Part D: J. Automob. Eng., Vol. 224.

Micheau, P., Bourassa, P., (2009), "Intermittent Predictive Steering Control as an Automobile Driver Model", J. of Dynamic Systems, Measurement, and Control, Vol. 131/021654-2.

Mirzae, M., Alizadeh, G., Eslamian, M., and Azadi, Sh., (2008), "An Optimal Approach to Nonlinear Control of Vehicle Yaw Dynamics", Proc. IMechE Part I: J. Syst. Control Eng. 222 (4), 217–229.

Mokhiamar, O., Abe, M., (2002), "Active Wheel Steering and Yaw Moment Control Combination To Maximize Stability as Well as Vehicle Responsiveness During Quick Lane Change For Active Vehicle Handling Safety", Proc. IMechE Part D: J. Automob. Eng., Vol. 216.

Moon, C., Choi, S.B., (2011), "A driver model for vehicle lateral dynamics", Int. J. Vehicle Design, Vol. 56, Nos. 1/2/3/4, pp.49-80.

Nam, k., Oh, S. , Fujimoto, H., Hori, Y., (2012), "Robust yaw stability control for electric vehicles based on active front steering control through a steer-by-wire system", International Journal of Automotive Technology, Volume 13, Issue 7 , pp 1169-1176.

Oliveira, P.S., Barros, L.S., Silveira Q. J., (2010), "Genetic Algorithm Applied to State Feedback Control Design", IEEE/PES Transmission and Distribution Conference and Exposition: Latin America.

Oscarsson, M., (2003), "Variable Vehicle Dynamics Design-Objective Design Methods", Master's thesis performed in Vehicular Systems. Reg nr: Lith-ISY-EX-3348.

Pacejka, H.B., (2002), "Tire and Vehicle Dynamics", Elsevier, Butterworth–Heinemann, Oxford.

Rahman, N., Alam, M.N., (2012), "Active vibration control of a piezoelectric beam using PID controller: Experimental study", Vol. 9, No. 6, 657 – 673.

Raksincharoensaka, P., Mizushimaa, T., Nagaia, M., (2010), "Direct Yaw Moment Control System Based on Driver Behaviour Recognition", Vehicle System Dynamics, 46: 1, 911-921.

Rosettes, E.J., (2003), "A Potential Field Framework for Active Vehicle Lane keeping Assistance", PhD Thesis, Stanford University.

Schoen, P.M., Hoover, R.C., Chinvorarat, S., and Schoen, G.M., (2009), "System Identification and Robust Controller Design Using Genetic Algorithms for Flexible Space Structures", J. of Dynamic Systems, Measurement, and Control, Vol. 131/ 031003-1.

Segel, L., (1982), "Basic Linear Theory of Handling and Stability of Automobiles", University of Michigan, International center for transportation studies.

Sharp, R.S., Casanova, D., Symonds, P., (2005), "A Mathematical Model for Driver Steering Control, with Design, Tuning and Performance Results", Vehicle System Dynamics, 33:289–326.

Tchamna, R., Youn, I., (2013), "Yaw rate and side-slip control considering vehicle longitudinal dynamics", International Journal of Automotive Technology, Vol. 14, No. 1, pp. 53–60.

Yang, H.H., (2010), "Driver Models to Emulate Human Anomalous Behaviors Leading to Vehicle Lateral and Longitudinal Accidents", The University of Michigan, PhD. thesis in Mechanical Eng.

Yang, X., Wang, Z., Peng, W., (2009), "Coordinated Control of AFS and DYC for Vehicle Handling and Stability Based on Optimal Guaranteed Cost Theory", Vehicle System Dynamics, 47: 1, 57-79.

Wei, Z., Guizhen, Y., Jian, W., Tianshu, S., Xiangyang, X., (2009), "Self-Tuning Fuzzy PID Applied to Direct Yaw Moment Control For Vehicle Stability", The Ninth International Conference on Electronic Measurement & Instruments.

Zakeri, J.A., Xia, H., Fan, J.J., (2009), "Dynamic responses of train-track system to single rail irregularity", Latin American Journal of Solids and Structures Vol. 6, 89-104.

Zhang, J.Y., Kim, J.W., Lee, K.B., and Kim, Y.B., (2008), "Development of an Active Front Steering (AFS) System With QFT Control", Int. J. of Automotive Technology, Vol. 9, No. 6, pp. 695−702.

Notations

Symbol	Definition	Symbol	Definition
$a(m)$	Front axle to C.G.	$t_s\ (s)$	Settling time
$b(m)$	Rear axle to C.G.	$U\ (m/s)$	Longitudinal speed
$C_{ss}\ (N/rad)$	Steering damping	u_{max}	Maximum Control Effort
C_{af}	Cornering stiffness of front tires combined	$V_y\ (m/s)$	Lateral speed
C_{ar}	Cornering stiffness of rear tires combined	$X_r(m)$	Mechanical trail
$E_d(s)$	Laplace transforms of preview tracking error	$y_d(m)$	Desired output trajectory
E_{ss}	Steady state error	$y_e\ (m)$	Lateral deviation
F_{wxi}	Longitudinal forces	$y_{ep}(m)$	Preview tracking error
F_{yf}	Lateral force of front axle	$a_i(rad)$	Tire slip angle
$F_{zi}\ (N)$	Tire vertical load	$\delta_f(rad)$	Steering angle
H	Proportional coefficient	$\delta_r(rad)$	Rear steering angles
$I_s(Kgm^2)$	Equivalent moment of inertia of steerable tires	Φ	Roll angle
$I_{sw}(Kgm^2)$	Equivalent moment of inertia of steering wheel	$\gamma_i(rad)$	Tire camber angle
k_d	Derivative gain	$\varkappa$	Real parts of closed-loop poles
k_i	Integral gain	λ_i	Tire longitudinal slip
k_p	Proportional gain	$\Delta(s)$	Laplace transforms of steering angle
$K_{ss}\ (Nm/rad)$	Steering stiffness	$\vartheta\ (m/s)$	Input steering wheel Angle
$L\ (m)$	Preview distance	$\psi\ (rad)$	Heading error angle
M_p	Overshoot	$\dot{\psi}\ (rad/sec)$	Road curvature rate
$M_z(N.m)$	Self aligning torque	τ_1	Derivative coefficient
N	Steering gear ratio	τ_2	Relocating during deviation
$R\ (m)$	Road curvature	τ_d	Delay times coefficient
$r\ (rad/sec)$	Yaw rate	τ_r	Reaction coefficient
$t_r(sec)$	Rise time		